

To: *PE&RS* Authors

From: Mike Renslow
Technical Editor

Thank you for using our online proofing process. On the pages following this letter, please find the PDF file for your paper being published in *Photogrammetric Engineering & Remote Sensing*.

Please examine this proof, make whatever corrections are necessary, and email the edited version to me (renslow76@comcast.net) as soon as possible. You may send your corrections using postal or delivery services to the address shown below.

Even though the proof is carefully studied by skilled proofreaders, an author can usually detect discrepancies which may be obscure to anyone else. This is particularly true in the case of equations and tables.

Please confine your corrections to errors in typesetting, spelling, etc., and refrain from making extensive changes or additions which are expensive to incorporate at this stage. You are allowed to make eight (8) changes to the proof; you may be charged for additional edits.

Please note that the quality of your PDF proof on screen, particularly the illustrations, depends on your computer equipment and software.

A “*PE&RS* Offprint Order Form” and “Assignment of Copyright to ASPRS” form are also attached in PDF format. Offprints must be ordered at this time so that they can be printed while the Journal is being printed. Both of the completed forms are to be returned to the Production Coordinator, ASPRS, 5410 Grosvenor Lane, Suite 210, Bethesda, MD 20814-2160 preferably by email (rkelly@asprs.org).

Sincerely,

Mike Renslow
Technical Editor - *PE&RS*
2880 Bailey Hill Road
Eugene, OR 97405
Tele: (541) 343-1066
E-mail: renslow76@comcast.net

Effect of Sun Elevation Angle on DSMs Derived from Cartosat-1 Data

Tapas R. Martha, Norman Kerle, Cees J. van Westen, Victor Jetten, and K. Vinod Kumar

Abstract

Along-track stereoscopic satellite data are increasingly used for automatic extraction of digital surface models (DSM) due to the reduced radiometric variation between the images. Problems remain with the quality of such DSMs, especially in steep terrain. This paper explores the accuracy of DSMs extracted from Cartosat-1 data acquired under high and low sun elevation angle conditions in High Himalayan terrain. The metric accuracy of the DSM was estimated by comparing it with check points obtained with a differential GPS. Additionally, we used spatial discrepancy of drainage lines to estimate errors in the DSM due to spatial autocorrelation. For valleys perpendicular to the satellite track, the DSM extracted from a low sun elevation angle data showed 45 percent higher spatial accuracy than the DSM extracted from high sun elevation angle data. The results indicate that the sun elevation angle and valley orientation affect the spatial accuracy of the DSM, though metric accuracy remains comparable.

Introduction

A digital elevation model (DEM) is one of the primary data sources for the study of earth surface processes. Contours from topographic maps, spot heights measured on the ground using total station or GPS, light detection and ranging (lidar) data, interferometric synthetic aperture radar (InSAR) data, aerial photos and satellite images are typical sources for DEM generation (Weibel and Heller, 1991; Li *et al.*, 2005; Smith *et al.*, 2006; Van Den Eeckhaut *et al.*, 2007). Techniques for DEM generation have been an active area of research for decades. Over the years, these techniques have been automated and new data sources were developed, most recently based on high resolution stereoscopic data from new satellite missions. Large scale automation and the emergence of new satellite data sources for the generation of

digital surface models (DSMs) necessitate accuracy testing before the data can be used for terrain analyses. The term DEM has been used widely in the literature as a generic descriptor for digital spatial representations of altitude. In fact, the terms DEM, digital terrain model (DTM), and DSM are often used as synonyms. However, when dealing with spatial digital representation of the Earth that include the objects above the surface, such as vegetation and man-made features, the term DSM should be used, whereas DTM is appropriate if the actual ground surface is represented. In this paper, we only use the term DEM in the generic discussion on elevation models.

In photogrammetric processing, the terrain elevation is computed from a satellite stereo pair by measuring the parallax between the two overlapping images. SPOT-5 HRS (high-resolution stereoscopic) data have been shown to be a valuable along-track stereoscopic data source for DSM generation (Toutin, 2006; Berthier and Toutin, 2008). Cartosat-1 and ALOS-PRISM are other, more recent, sources of along-track stereoscopic data, with the potential for easier and more accurate DSM generation. They offer considerable advantages compared to across-track methods, such as employed by the SPOT-1 through SPOT-4 and IRS-1C/D satellites, which are frequently affected by atmospheric differences between the images. Cartosat-1, launched in May 2005 by the Indian Space Research Organisation (ISRO), is a global mission designed to acquire high-resolution stereoscopic images for cartographic application, urban development, and disaster management (NRSC, 2006). It is the first satellite in the along-track category with 2.5 m spatial resolution. Cartosat-1 has several distinct features, such as unique sensor geometry, 10-bit radiometric resolution, rational polynomial coefficients (RPC), on-demand tilting capability, and a five day revisit period with dedicated stereoscopic cameras, making it a suitable choice for DSM generation in any part of the world. Cartosat-1 has two panchromatic cameras, PAN-Aft and PAN-Fore, with an off-nadir viewing angle of -5° and $+26^\circ$, respectively. The images of the same scene are acquired at a time difference of 52 seconds (Radhika *et al.*, 2007), minimizing radiometric differences. Images are acquired with a base to height ratio (B/H) of 0.62, which is within the suitable range specified by Light *et al.* (1980) for topographic mapping. Detailed technical specifications of Cartosat-1 are available in NRSC (2006).

The availability of DEMs from global datasets has given rise to new applications (Murphy and Burgess, 2006; Ehsani

Tapas R. Martha is with Geosciences Division, National Remote Sensing Centre (NRSC), Indian Space Research Organisation (ISRO), Hyderabad - 500625, India, and formerly with Department of Earth Systems Analysis, International Institute for Geo-Information Science and Earth Observation (ITC), Enschede, The Netherlands. (tapas_martha@nrsc.gov.in).

K. Vinod Kumar is with Geosciences Division, National Remote Sensing Centre (NRSC), Indian Space Research Organisation (ISRO), Hyderabad - 500625, India.

Norman Kerle, Cees J. van Westen, and Victor Jetten are with Department of Earth Systems Analysis, International Institute for Geo-Information Science and Earth Observation (ITC), Hengelosestraat 99, 7500 AA, Enschede, The Netherlands.

Photogrammetric Engineering & Remote Sensing
Vol. 76, No. 4, April 2010, pp. 000–000.

0099-1112/10/7604-0000/\$3.00/0
© 2010 American Society for Photogrammetry
and Remote Sensing

and Quiel, 2008) and also widened its user community. Also due to commercial off-the-shelf (COTS) software tools, the data are increasingly used by non-photogrammetrists. However, assessing the accuracy of DEMs has always been difficult (Gooch *et al.*, 1999; Gong *et al.*, 2000). While traditional airborne photogrammetric projects covered comparatively small areas and typically used differential GPS (DGPS) to provide needed ground control, satellite-based photogrammetry covers vast areas without the strict need for GPS observations. Particularly, but not exclusively, for non-photogrammetrist assessing the accuracy of the derived data is a substantial challenge. Unfortunately, also commercially generated DEMs contain little information on the error distribution (Holmes *et al.*, 2000). Some standards exist for assessing the absolute accuracy of DEMs. According to FGDC (1998), a minimum of 20 check points is required for calculating the accuracy. Höhle and Potuckova (2006) of the European Spatial Data Research (EuroSDR) group suggested that DTM accuracy assessment methods should be universal, and the reference check points should have accuracies at least three to five times better than the error metrics of the DTM. Although stereoscopic data from new generation along-track satellites are able to generate high-resolution DSMs in a more robust and sophisticated manner, principally through the use of RPCs, the challenge remains to assess their accuracy. DEM accuracy is typically expressed through the root mean square error (RMSE) of the elevation, calculated by comparing sampled elevation points of the produced DEM with independent ground control points (GCP). This does not, however, result in a representative accuracy figure, as the RMSE is based on only a limited number of points, whereas the DEM contains thousands to millions of elevation points, and thus conveys nothing about the actual error distribution, and little about the accuracy in the vast parts of the DEM where no ground truth exists. In recognition of the limitations of using a small number of GCPs for accuracy assessment, a DEM with higher resolution and better quality can be used as a reference (Bolstad and Stowe, 1994; Gorokhovich and Voustianiouk, 2006). However, suitable reference DEM data are typically not available.

We selected an area in steep, mountainous terrain, where topographic shadows are likely to have a critical effect on photogrammetric DSM generation, a problem we investigate by using recently developed satellite image precision processing (SAT-PP) software (Zhang and Gruen, 2006). In addition to global accuracy assessment using independent check points, we also test the reliability of those values using the models developed by Aguilar *et al.* (2007).

According to Aguilar *et al.* (2005) and Chaplot *et al.* (2006), DEM inaccuracies result from errors in the source data, interpolation method, sampling density, and are also more prominent for steep terrain surfaces. However, in addition, errors in a DEM can also be a function of the viewing direction of the sensor, the valley orientation and the sun elevation angle, effects that have not been studied to our knowledge. In this paper, along-track stereoscopic Cartosat-1 data acquired in summer and winter seasons of an area in the High Himalayas were analyzed to evaluate the accuracy of DSMs as a result of different sun elevation angle conditions and variable valley orientation. Thus implicitly we also consider the effect of local sensor orientation.

Errors in elevation data can have different facets, and therefore, a comprehensive assessment of these possible errors is needed. For example hydrologists and geomorphologists may be less concerned about absolute accuracy, but more about DEM derivatives, such as slope, aspect, or curvature (Wise, 2007). However, conceptual challenges persist, e.g., how to compare aspect and slope values from

different resolution DEMs, or indeed how to measure those values accurately in the field. Particularly in high-relief terrain, this scale-dependency of derivatives poses immense difficulties. The importance of accuracy assessment of such DEM derivatives has been emphasized by previous workers (Bolstad and Stowe, 1994; Wise, 2000; Chaplot *et al.*, 2006). Wise (2000) used drainage lines to investigate the effect of different DEM interpolation methods and consequences for hydrological applications. Similarly, Holmes *et al.* (2000) investigated DEM error distributions in 30 m USGS elevation data using statistical measures, and how these errors propagate into derivatives such as drainage networks. Endreny *et al.* (2000) assessed the effect of errors in DEMs derived through satellite photogrammetric methods on entire stream networks and basin boundaries. In this paper we invert this approach by using the drainage network as a proxy in the actual DEM accuracy assessment, a novel departure from previous studies.

Automatic DSM Generation

Stereoscopic satellite images are acquired either along or across the track. Satellite photogrammetry using multi-date across-track data first became a viable method for DSM extraction in the 1980s with the availability of SPOT-1 (Kratky, 1989) and IRS-1C/1D data (Malleswara Rao *et al.*, 1996; Bahuguna *et al.*, 2004). However, the difficulty in obtaining cloud free across-track stereo data over large areas prompted the development of a stereo system using along-track images acquired nearly simultaneously (Hirano *et al.*, 2003). This reduces the radiometric variation between the two images of a stereo pair and leads to the extraction of more accurate elevation data (Toutin, 2004a; Radhika *et al.*, 2007).

Toutin (2001) gives a detailed description of the methods of DEM extraction from satellite visible and infrared data. An important step in this process is the calculation of elevation parallax for conjugate points. Image matching in mountainous areas frequently fails as a result of shadow or poor contrast in areas of snow, glaciers or homogenous vegetation. Due to different viewing angles of the two cameras in Cartosat-1, steep slopes are also frequently occluded, depending on the steepness of the slope; similarly, the extent of shadow depends upon the sun elevation angle (Figure 1). Another cause for the partial failure of image matching of along-track stereo pairs in such areas is the relative distortion of features between the two images (Eckert *et al.*, 2005). In such cases, image matching produces inaccurate, less dense, and irregularly distributed match points. According to Bahuguna *et al.* (2008) problems in image matching due to steep terrain result in an inaccurate DEM, even with appropriate B/H ratio. Other common problems of image matching for automatic DSM generation are listed by Zhang and Gruen (2006). A list of COTS software for extraction of DEM from stereoscopic data is given by Toutin (2008). These software packages employ various matching algorithms, and should be selected with respect to the data to be used and the terrain characteristics.

A rational function model (RFM) is an alternative to a physical sensor model that facilitates photogrammetric processing of satellite data (Tao and Hu, 2002). The RFM allows users to perform orthorectification and 3D extraction from imagery without having knowledge of the sensor model, and the accuracy of the 3D model can be increased with additional GCPs (Hu and Tao, 2002). The RFMs are generated from onboard instruments, in particular GPS and improvised star sensors, and are provided by the data vendor (Sadasiva Rao *et al.*, 2006). RPCs are determined from RFM and provided to the end user for DSM generation. Since RPCs are terrain independent, they require refinement at scene/block level.

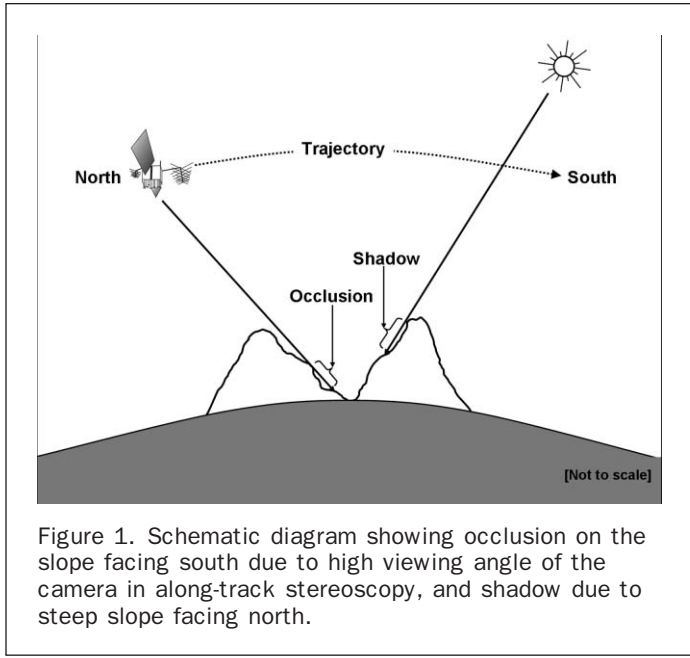


Figure 1. Schematic diagram showing occlusion on the slope facing south due to high viewing angle of the camera in along-track stereoscopy, and shadow due to steep slope facing north.

Refinement of the orientation result obtained using Cartosat-1 RPC at scene/block level with GCPs can produce a DSM of about four meter vertical accuracy (Ahmed *et al.*, 2007). So far there is no consensus on the optimum number of GCP(s) required for extracting a sufficiently accurate DSM from Cartosat-1 data. Sadasiva Rao *et al.* (2006) observed that one control point is adequate for restitution of the Cartosat-1 model. However, according to Baltasvias *et al.* (2007) the distribution of GCPs (planimetric and vertical) is crucial to achieve high accuracy, and they recommended that a minimum of six GCPs should be used for a Cartosat-1 scene.

Study Area

The study area is a part of the Mandakini River Valley in the High Himalayas, located around the town of Okhimath in the Rudraprayag District of Uttarakhand State, India (Figure 2). The center coordinates of the study area are 30° 30' 48" N and 79° 05' 41" E. Okhimath is situated at an average elevation of 1,300 m at the confluence of the Mandakini and Madhyamaheshwar Rivers. The Mandakini River is a tributary to the Ganges River, one of the largest river systems in the world. The elevation ranges from 718 m to 4,510 m with highly variable terrain relief and land-cover. The northeastern part of the area is always snow covered. This area is dominated by low altitude oak forest, which does not shed its leaves seasonally. Therefore, the vegetation surface commonly does not change, and is discarded as a potential reason for DSM differences in this paper. The terrain is dominantly steep and rugged with few flat fluvial terrace areas along the Mandakini River. Since the rugged topography is controlled by the geological structure, there are many fault-related, south-facing escarpments in this area. The northeastern and western parts of the area are very difficult to access.

Methods

DGPS Survey

The DGPS survey was carried out using three GPS receivers, one located at the base station, operated continuously throughout

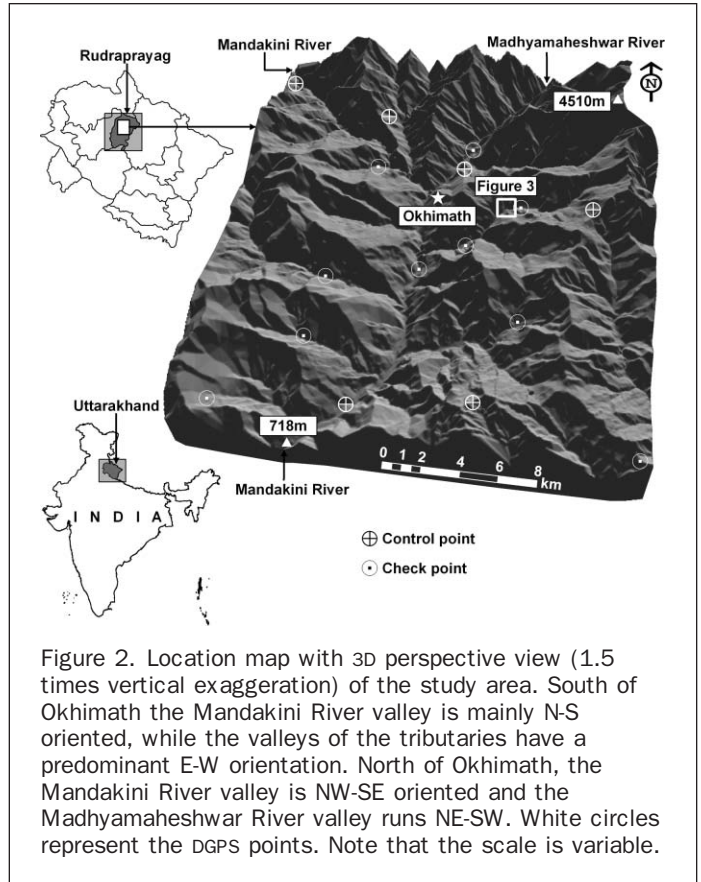


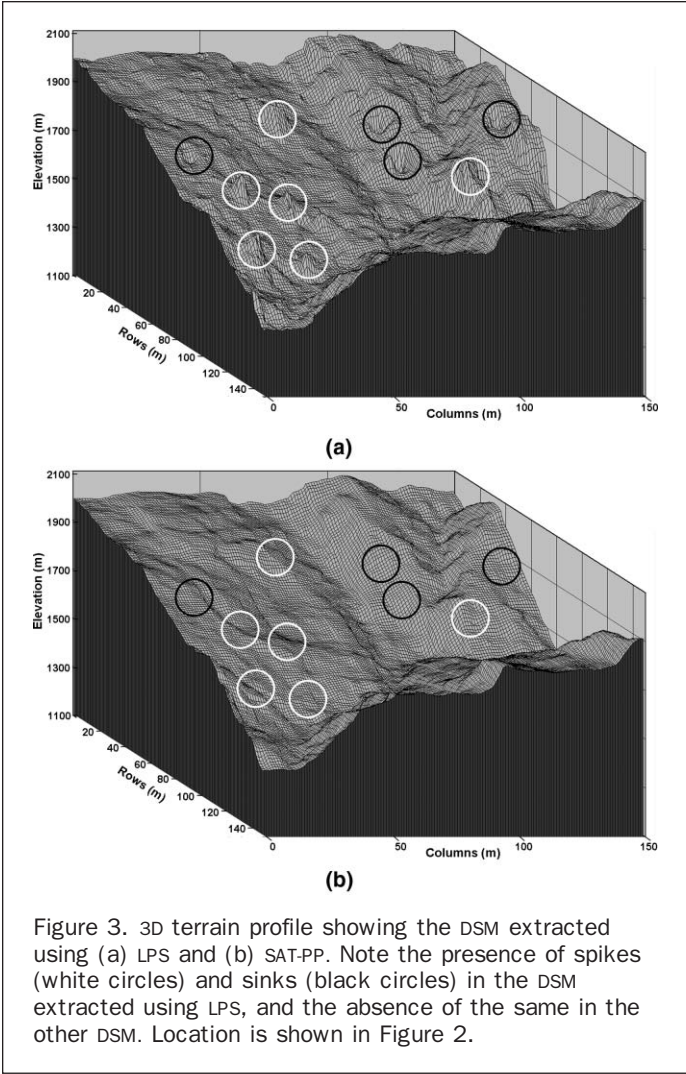
Figure 2. Location map with 3D perspective view (1.5 times vertical exaggeration) of the study area. South of Okhimath the Mandakini River valley is mainly N-S oriented, while the valleys of the tributaries have a predominant E-W orientation. North of Okhimath, the Mandakini River valley is NW-SE oriented and the Madhyamaheshwar River valley runs NE-SW. White circles represent the DGPS points. Note that the scale is variable.

the survey period, and the remaining two used as rovers to collect ground coordinates in the study area. A Leica SR 520 dual frequency (L1 and L2) receiver was used in the DGPS survey. The DGPS survey in this steep mountainous area was challenging because of terrain inaccessibility, difficulty in identifying ground points, and narrow valleys restricting the satellite signal for the receiver. However, by taking systematic traverses along the accessible routes, 16 points were collected, with a fairly good planimetric and vertical distribution across the scene (Figure 2). Postprocessing of the data recorded in the GPS receivers was carried out using Leica GeoOffice software to calculate the coordinates of the ground control points. The standard deviation of the errors of elevation, longitude, and latitude of the points obtained from the DGPS survey range between 0.10 m to 0.46 m, 0.04 m to 0.15 m, and 0.04 m to 0.21 m, respectively.

Processing of Cartosat-1 Data

Two sets of stereoscopic Cartosat-1 data were processed: one from a summer season (06 April 2006) with a high sun elevation angle (62°), and the other from a winter season (01 December 2005) with a low sun elevation angle (38°). We first used Leica Photogrammetric Suite (LPS) to process the data. Despite optimization and adaptation of the extraction strategy, the resulting DSM contained spurious spikes and sinks, an artifact frequently reported in previous studies (Gooch and Chandler, 2001; Gooch *et al.*, 1999; Kerle, 2002).

Manual removal of such spikes and sinks can be attempted, but despite being time-consuming, it can only be accurately done with additional data or extensive stereoscopic assessment of the source image data. Instead, SAT-PP photogrammetric software was used to re-process the data, and the resulting DSMs were found to have

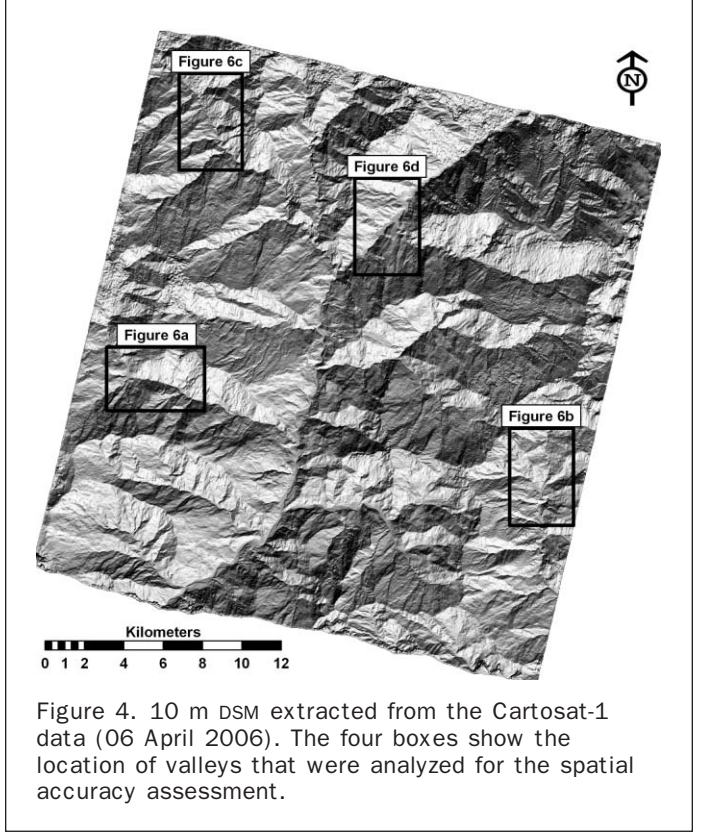


virtually no spikes and sinks (Figure 3). SAT-PP was developed by the Institute of Geodesy and Photogrammetry of ETH Zurich for photogrammetric processing of high-resolution images. Unlike LPS, it not only uses a template matching technique, but incorporates an additional edge-matching strategy. It is capable of generating DSMs and orthoimages with pixel level accuracy (Gruen *et al.*, 2007). The general steps of SAT-PP processing of stereoscopic images are: (a) image pre-processing, (b) multiple primitive multi-image matching, and (c) refinement of matching by least squares method. Details of these methods are explained in Zhang and Gruen (2006). The advanced matching approach is based on combining matching results of feature points, grid points, and edges (Zhang and Gruen, 2006). The approach is robust and has been reported to result in 75 percent matching success for high-resolution stereo pairs even in steep mountainous areas (Zhang and Gruen, 2006). It accounts for both grayscale and geometric differences of features on the ground, thus making it especially useful for mountainous terrain.

We used six GCPs as control points to refine the orientation result of the RPC model during the processing of Cartosat-1 data from both seasons. The RMSEs of the residuals obtained after the block triangulation are given in Table 1. We generated DSMs with 10 m grid size (Figure 4), and

TABLE 1. RMSE OF CONTROL POINT RESIDUALS AFTER BLOCK TRIANGULATION

Elevation model	RMSE _x (m)	RMSE _y (m)	RMSE _z (m)
<i>AprCartoDSM</i>	0.874	0.781	0.465
<i>DecCartoDSM</i>	0.599	0.392	0.972



labeled them as *AprCartoDSM* and *DecCartoDSM* for 06 April 2006 and 01 December 2005, respectively.

Accuracy Assessment

We calculated the following statistical parameters for global accuracy assessment of the DSMs: RMSE (Aguilar *et al.*, 2005), range, mean error (μ), and standard deviation error (σ) (Li *et al.*, 2005). Although RMSE is widely used for DEM accuracy assessment, its limitation has also been highlighted (Florinsky, 1998; Wise, 2000). Westaway *et al.* (2001) suggested that mean error is the true measure of global accuracy, as it reflects any systematic bias in the DEM with the standard deviation showing the error distribution. We calculated these parameters by comparing the checkpoints between the produced and reference data. The checkpoints measured on the ground by DGPS survey are used as reference for comparison. The equations to calculate these errors are given below:

$$\text{Range} = e_{\max} - e_{\min} \quad (1)$$

$$\text{RMSE} = \sqrt{\frac{\sum_{i=1}^n (Z_i^{\text{dsm}} - Z_i^{\text{ref}})^2}{n}} \quad (2)$$

$$\mu = \frac{1}{n} \sum_{i=1}^n (Z_i^{dsm} - Z_i^{ref}) \quad (3)$$

$$\sigma = \sqrt{\frac{\sum_{i=1}^n (e_i - \mu)^2}{n - 1}} \quad (4)$$

where Z^{dsm} is elevation of the DSM, Z^{ref} is elevation from reference data, n is number of points, and e_{max} and e_{min} are the maximum and minimum errors, respectively, obtained by comparing the checkpoints from the DGPS survey with the DSM.

In order to estimate the spatial pattern of errors in the DSM, and thus to address DEM accuracy in a more comprehensive way, we used drainage lines as an accuracy proxy. Drainage lines were derived manually from the Cartosat-1 data of 06 April 2006 and 01 December 2005 using a feature extraction tool in LPS. They were used as reference, and compared against the drainage lines extracted automatically from the DSMs using the FLOWACCUMULATION algorithm of ArcGIS®. Prior to that, spurious depressions in the DSMs were eliminated with a FILL function to make it hydrologically correct (Murphy *et al.*, 2008). During automatic drainage extraction, a 50,000 m² area threshold was selected in order to restrict the extraction of some first order drainages, as the corresponding reference drainages were difficult to demarcate through 3D visualization.

We compared the drainage lines for their degree of mismatch, adapting a method of Carrara *et al.* (1992) developed to compare spatial discrepancy of two landslide inventory maps. Using this method, we compared the closeness of the automatically extracted drainage line with the standard reference drainage line. A buffer of 30 m around the drainage lines was calculated in GIS to prepare the area of influence (Figure 5). Since a 3 × 3 pixel window was used in the automatic drainage extraction algorithm, we used a buffer distance of 30 m (three times the DSM resolution) on both sides of the drainage lines. An error index (EI) was calculated using the following formula.

$$EI = \frac{A_2 - (A_1 \cap A_2)}{A_1} \quad (5)$$

where A_1 is the area of the reference drainage buffer, A_2 is the area of the drainage buffer extracted from the DSM, and $A_1 \cap A_2$ is the common area between the two drainages. EI ranges between 0 to 1, with lower values signaling a higher degree of match of the drainage lines.

Effect of Valley Orientation

Although along-track stereoscopic images are increasingly used for DSM generation, similar to across-track viewing there are limitations when the DSM is generated for steep mountainous areas due to the viewing angle of the cameras. Since Cartosat-1 data are acquired in the descending mode, the PAN-Aft camera cannot view a terrain with slopes greater than 85° and northerly aspect, and the PAN-Fore camera cannot view a terrain with slopes greater than 64° and southerly aspect (Radhika *et al.*, 2007). The relative compression and elongation of features in the image is a function of slope of the terrain in the along-track direction of the satellite (Radhika *et al.*, 2007). It means that in the along-track stereoscopic data this problem will predominantly occur on slopes with both south and north aspects, i.e., E-W oriented valleys, where we can expect image matching problems. Conversely, for N-S valleys, image distortion is expected to be minimal. Radhika *et al.* (2007) reported good image matching results for Cartosat-1 data for slopes ranging from -30° (direction opposite to the satellite motion, i.e., north facing) to 10° (in the same direction of the satellite motion, i.e., south facing). It means that slope and orientation of the valley, with reference to the satellite track, do influence the spatial accuracy of the DSM.

To evaluate this effect, an experiment was performed by considering four principal types of main valley orientation i.e., E-W, N-S, NW-SE, and NE-SW. Drainage lines, an important characteristic of valleys, were used to evaluate the spatial accuracy of the DSMs. The distribution of the valleys in the study area (Figure 4) offers an ideal opportunity to evaluate the effect of their orientation on DSM extraction in four major directions.

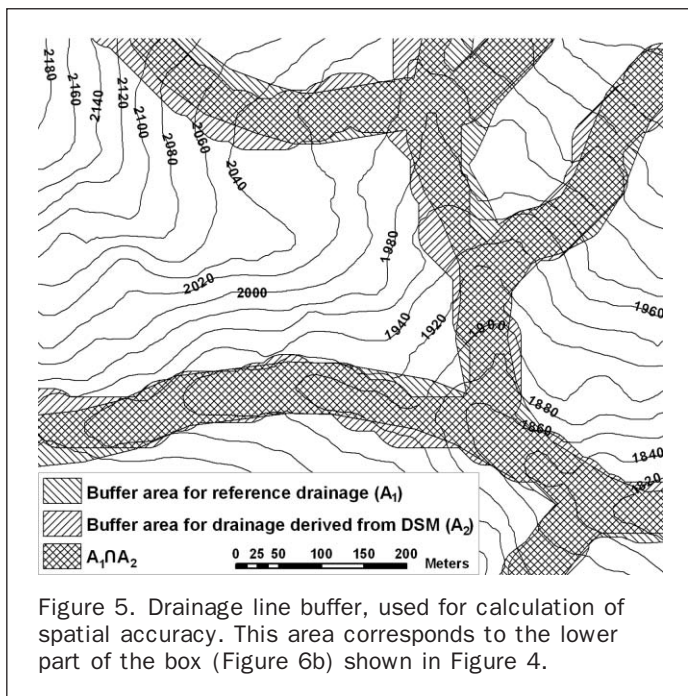


Figure 5. Drainage line buffer, used for calculation of spatial accuracy. This area corresponds to the lower part of the box (Figure 6b) shown in Figure 4.

Results

DSM Global Accuracy

The vertical and planimetric accuracies of the AprCartoDSM and DecCartoDSM were estimated using ten independent check points, resulting in vertical RMSEs for both DSMs nearly identical to the spatial resolution of the image (Table 2).

To verify the reliability of the DSM global accuracy values shown in Table 2, we followed the theoretical approach developed by Aguilar *et al.* (2007), because of the non-Gaussian distribution of elevation residuals for this area. The two models developed by Aguilar *et al.* (2007) estimate the reliability of the global statistical measures as a percentage by calculating the standard deviations of σ and RMSE, with lower values indicating higher reliability. The models were applied to the residual dataset and the results are shown in Table 3.

Effect of Valley Orientation on DSM Accuracy

Spatial accuracy assessment of the DSMs extracted from the two Cartosat-1 datasets with high and low sun elevation angles was carried out by calculating the degree of match between the reference and automatically extracted drainage lines. Two reference drainage systems (from the April and December images), when compared, showed negligible

TABLE 2. STATISTICAL ASSESSMENT OF THE GLOBAL ACCURACY OF DSMs USING TEN CHECKPOINTS; X AND Y SHOW THE PLANIMETRIC, AND Z THE VERTICAL ACCURACY

Variables	Statistical parameters (Errors)	<i>AprCartoDEM</i> (m)	<i>DecCartoDEM</i> (m)
X	Minimum	0.02	0.02
	Maximum	1.14	1.46
	μ	0.60	0.27
	RMSE	0.71	0.48
	σ	0.40	0.44
Y	Minimum	0.03	0.02
	Maximum	0.93	0.46
	μ	0.46	0.15
	RMSE	0.58	0.21
	σ	0.37	0.16
Z	Minimum	0.12	0.10
	Maximum	4.98	5.80
	μ	1.27	0.96
	RMSE	2.31	2.51
	σ	1.99	2.02

TABLE 3. RELIABILITY OF THE VERTICAL GLOBAL ACCURACY OF BOTH THE DSMs

DSM	Reliability of σ (%)	Reliability of RMSE (%)
<i>AprCartoDEM</i>	22.1	23.4
<i>DecCartoDEM</i>	34.2	37.5

mismatch. We selected valleys for the required orientations with comparatively little topographic shadow in both datasets. It was observed that for an E-W valley, the main valley drainage lines extracted from *AprCartoDSM* showed significant spatial deviation from the reference drainage line (Figure 6a1). Surprisingly, the main valley drainage derived from *DecCartoDSM* showed a better match ($EI = 0.35$) with the reference drainage (Figure 6a2) than those from *AprCartoDSM* ($EI = 0.64$). For the remaining three types of valley orientation (N-S, NW-SE, and NE-SW), no significant deviations of drainage lines were observed between both DSMs (Figures 6b1 and b2, c1 and c2, d1 and d2).

Steep hill slopes are the probable areas for failure of image matching in *Cartosat-1* (Radhika *et al.*, 2007). Therefore, DSM portions in those areas are more prone to error than the main valley floor. To know precisely the areas of good degree of match, we divided the drainage lines into two categories: one corresponding to the main valley (one drainage line in the central part of the valley), the other corresponding to hill slopes. The EI was calculated using Equation 5.

Effect of Shadow on DSM Generation

Shadow is a homogeneous area in the image, and automatic image matching mostly fails in such areas resulting in elevation values in these areas that are incorrect due to poor interpolation from the sparsely distributed surrounding match points. The extent of topographic shadow depends on the steepness of the terrain, valley orientation, and sun elevation angle. In the area studied in this paper, some parts with a steep slope and north aspect are under more shadow in the winter season data than the summer season. For example, the small part of the valley shown in Figure 7 is 51 percent under shadow in the winter season data, compared to only 2 percent in the summer season data. Hence, differences in the distribution and density of match points were observed for the data of both seasons

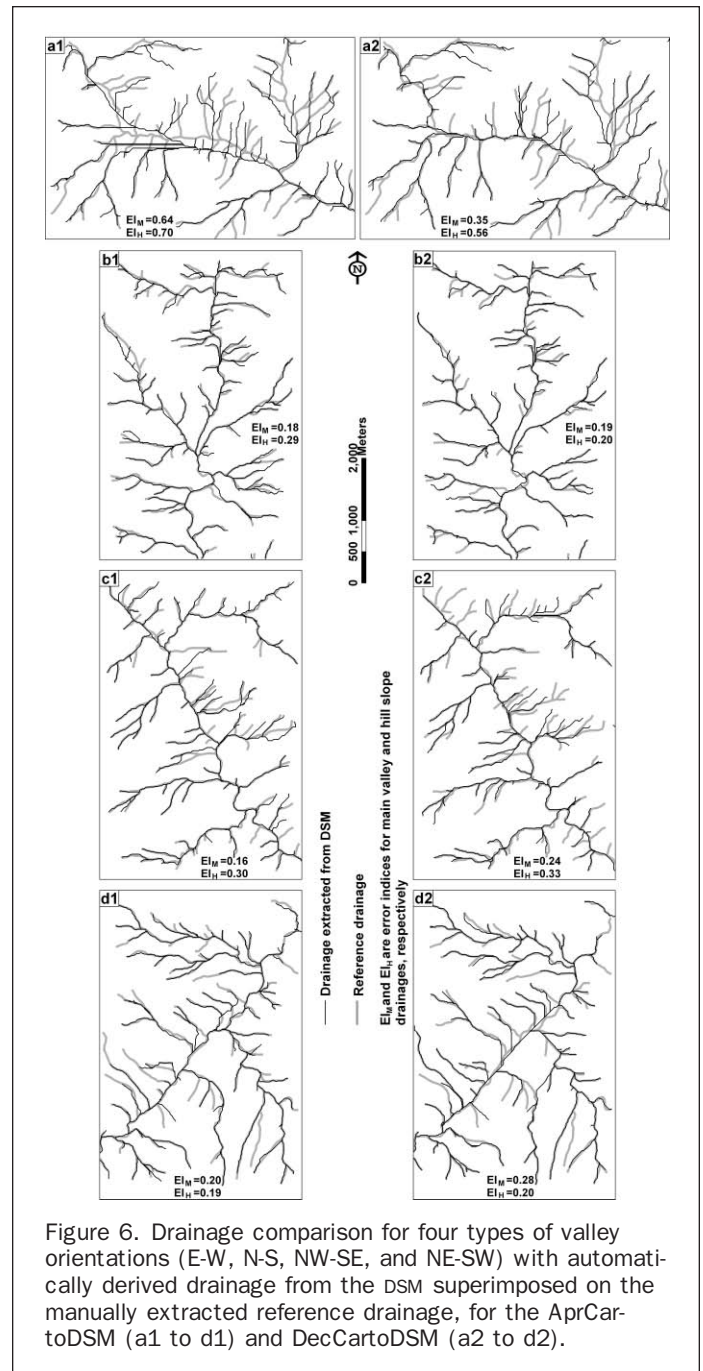


Figure 6. Drainage comparison for four types of valley orientations (E-W, N-S, NW-SE, and NE-SW) with automatically derived drainage from the DSM superimposed on the manually extracted reference drainage, for the *AprCartoDSM* (a1 to d1) and *DecCartoDSM* (a2 to d2).

(Figure 7a and 7b). The density of match points was lower for the winter season data than the summer season data around the areas affected by shadow. A terrain profile of the area shows significant differences in elevation (Figure 7c). For areas that are not under shadow the match points were generated evenly and there was no significant difference of elevation in the two DSMs (Figure 7c).

Discussion

DSMs for a steep mountainous area were extracted from *Cartosat-1* stereo pairs of both summer and winter seasons using SAT-PP. This software proved to be robust for automatic DSM extraction due to its superior image matching

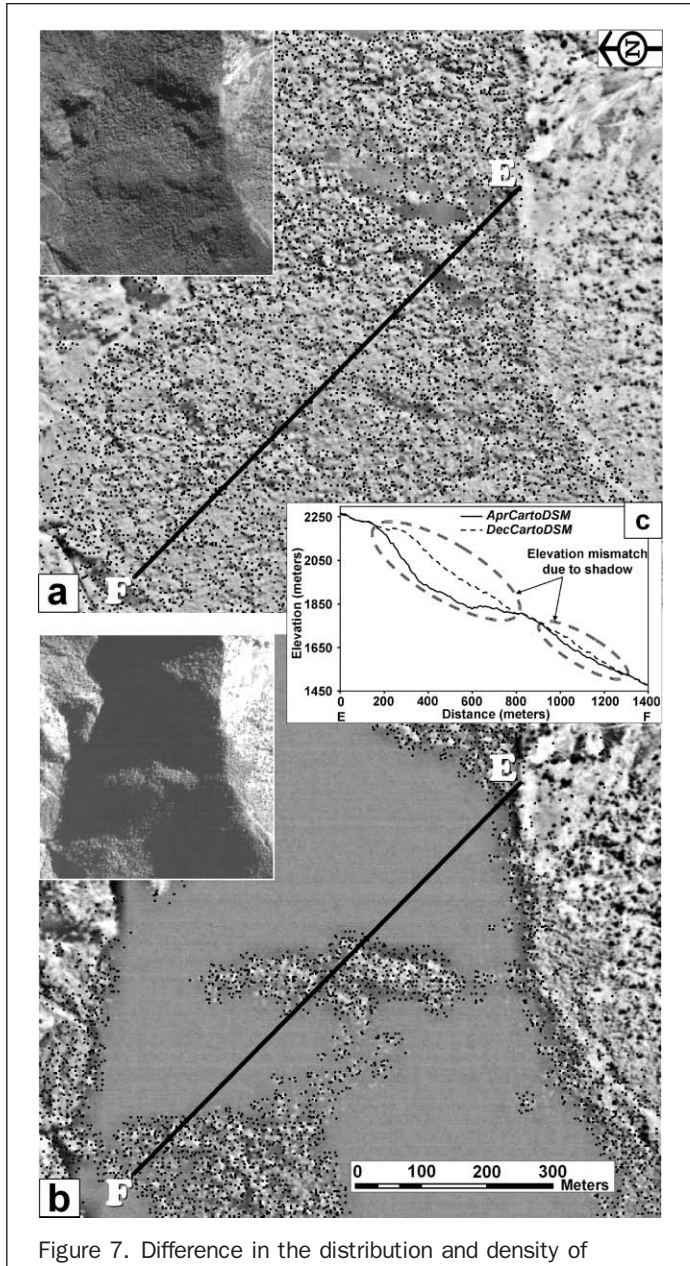


Figure 7. Difference in the distribution and density of matched points (black dots) in shadow areas from Cartosat-1 images of (a) 06 April 2006 and (b) 01 December 2005. E-F profile in (c) shows the difference of elevation in shadow affected areas; (a) and (b) have the same scale and orientation. The insets in (a) and (b) show the shadow conditions. The image contrast is reduced to highlight the distribution of points.

algorithm (based on feature points, grid points, and edges), as compared to LPS.

A high level of global accuracy was achieved due to the use of additional GCPs for refining orientation result of the RPC model (Table 2). It was better than previously reported for Cartosat DSMs by Ahmed *et al.* (2007) due to better planimetric and vertical distribution of control points used for triangulation of our datasets. No significant differences in vertical and planimetric RMSEs between the two DSMs were observed (Table 2). However, the reliability of global accuracy values for AprCartoDSM is better than the DecCartoDSM

(Table 3). Reliability of global accuracy values is a function of the number of checkpoints. For example, Aguilar *et al.* (2007) obtained a good reliability value of 6.3 percent when a sample size of 128 check points was used. The overall reliability of the two DSMs generated in this study must be considered unsatisfactory by the Aguilar *et al.* (2007) measure, a result of the low number checkpoints available. Local errors were also observed in the DecCartoDSM due to the presence of shadow (Figure 7c). This is due to lack of contrast in the shadow areas, which leads to absence of matched points.

Apart from the terrain steepness, orientation of valleys with respect to satellite track is another important factor in along-track stereoscopy that has a significant effect on the DSM spatial accuracy. According to Radhika *et al.* (2007), image matching is a function of slope along the direction of satellite track in Cartosat-1. This means that E-W valleys are problematic areas for image matching, as the variation of slope is mainly in the along-track direction. Conversely, we can expect minimum problems for image matching in N-S valleys. We found maximum EI values for the main valley and hill slope drainages along E-W oriented valleys, in comparison to the three other types of orientations (Figure 6). Further, in the E-W valley, the spatial accuracies of the main valley drainage from both DSMs are better when compared to the hill slope drainage (Figure 6). This difference in spatial accuracy is due to limited variation of slope along the valley floor than, as compared to high variation in the hill slopes areas. Therefore, overall lower spatial accuracy for E-W oriented valleys than for other orientations can be attributed to image matching problem.

In the Himalayas, geological structure has a strong influence on shaping the topography. The valleys and ridge lines mostly follow geological structure. We observed that the drainage lines in an E-W valley were better matched on hill slopes facing north than the drainage lines on the hill slopes facing south (Figure 6a1 and 6a2). This is due to the typical topography of this area as shown in Figure 8, where hill slopes facing north are gentle and hill slopes facing south are steep.

The spatial accuracy of the main valley and hill slope drainages extracted from the DecCartoDSM are 45 percent and 20 percent higher than the AprCartoDSM for E-W valleys, respectively. This is a result of a higher number of

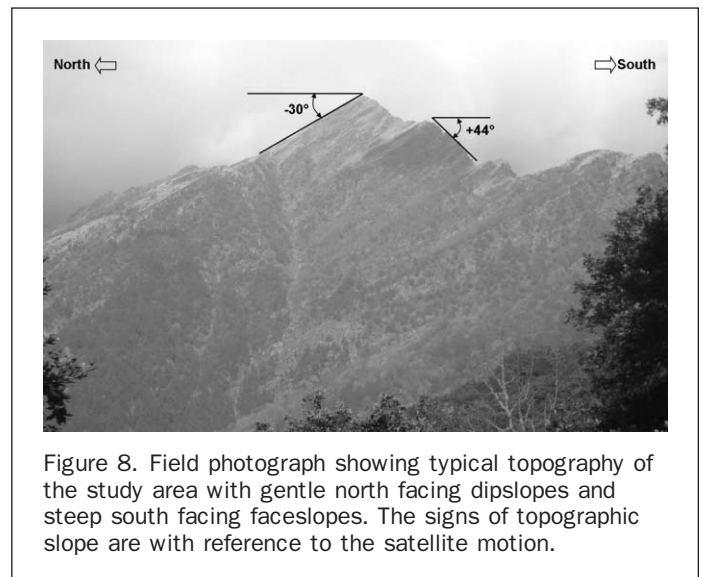


Figure 8. Field photograph showing typical topography of the study area with gentle north facing dipslopes and steep south facing faceslopes. The signs of topographic slope are with reference to the satellite motion.

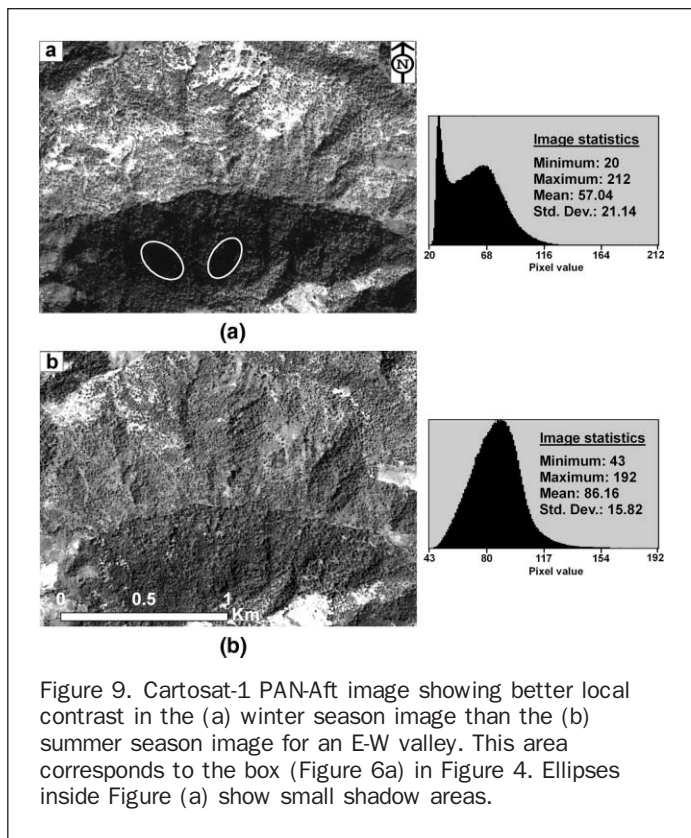


Figure 9. Cartosat-1 PAN-Aft image showing better local contrast in the (a) winter season image than the (b) summer season image for an E-W valley. This area corresponds to the box (Figure 6a) in Figure 4. Ellipses inside Figure (a) show small shadow areas.

match points generated in the valley floor and hill slope portions of the E-W valleys for winter season data than the summer season data. When analyzing the pixel information, we found a good local contrast in the winter image compared to the summer image (Figure 9), meaning that radiometric variation is better in the winter than the summer season data, even though land-cover remains the same. The image shows a higher range and standard deviation in the winter than the summer season data (Figure 9), and explains the presence of more match points in the former, as most image matching algorithms rely on strong local contrast (e.g., Kerle, 2002). Better radiometric variation in the winter season data may be due to proper illumination of the hill slopes, particularly those facing south by the sun with a low elevation angle. Although shadow is seen in the north facing slope of the winter season image (Figure 9a), these are small pockets (ellipses in Figure 9a), embedded in less intensively but sufficiently illuminated areas for SAT-PP to identify match points unlike in the area shown in Figure 7b, where the DN-value range within the shadow areas was too low, and the shadow area too extensive, resulting in blanket interpolation.

Conclusions

In this paper, we generated two DSMs using high and low sun elevation angle Cartosat-1 data for a steep mountainous area in the Himalayas, and assessed the advantages and limitations of these stereoscopic images as a source of elevation data. High-resolution, along-track stereoscopic data, such as from Cartosat-1, have become a major source for DSM generation. GCPs were used to refine the orientation result of the RPC model of Cartosat-1 data and resulted in a DSM with a vertical RMSE equivalent to the spatial resolution

of the images, although this also reflects a relatively low number of GCPs largely confined to less steep areas that we would expect to be more accurate in the resulting DSM. The RMSEs were found to be comparable for AprCartoDSM and DecCartoDSM with 23.4 percent and 37.5 percent reliability, respectively. These results are lower than previously reported results (e.g., Aguilar *et al.*, 2007; Li, 1991), due to the lower number of independent checkpoints available. However, local errors exist in the DSM in shadow areas that result from low sun elevation.

Apart from the metric accuracy, spatial accuracy of the DSMs was estimated by comparing automatically extracted drainage lines from the DSM with reference drainage information. We found that valley orientation has a significant effect on the planimetric as well as vertical accuracy of a DSM extracted from along-track stereoscopic data. The minimum and maximum spatial accuracies were obtained for E-W and N-S oriented valleys, respectively. This information is of use for hydrologists and geomorphologists when anticipating potential error sources, since the inaccuracies primarily affect commonly used DSM derivatives.

Although it is commonly assumed that a high sun elevation angle (less topographic shadow) is favorable for automatic DSM generation, we found that for E-W oriented valleys the DSM extracted from low sun elevation angle data provides better spatial accuracy than the DSM from data captured under a high sun elevation angle, if the actual valley is sunlit in both datasets. This effect can be seen in the area shown in Figure 7b, where extensive shadow resulted in blanket interpolation, versus the slope shown in Figure 9a where smaller shadow pockets led to spatially confined DSM errors. However, the effect of illumination needs to be studied in more detail.

Both results are important for DEM users as they show that the sun elevation angle and local valley orientation can have a pronounced effect on the accuracy of a DSM, yet the consideration of these parameters is typically neglected. Our method of spatial accuracy assessment is simple and can be adopted by a DEM user, as it does not require a reference DEM which in most cases is unavailable. It will be interesting to evaluate the effect of valley orientation and sun elevation angle on the spatial accuracy of DSMs derived from other along-track data sources with similar sensor configuration, such as ALOS-PRISM and SPOT-5 HRS.

Acknowledgments

This paper is the outcome of the research carried out under the framework of GSI-NRSC-ITC joint collaboration. The encouragement by the Director, NRSC, and Dr. P.S. Roy, Deputy Director, RS&GIS-AA, NRSC is duly acknowledged. For the DGPS survey, we are thankful to Dr. Raghu Venkataraman, GM, NRSC for his support, and to Mr. Anantha Padmanabha, Mr. M. Mohan Naidu, and Mr. N. Satyanarayana for the field survey. We are indebted to Professor Armin Gruen and Dr. Devrim Akca, ETH Zurich, for providing the SAT-PP software and support for processing the stereo data. We also thank three anonymous reviewers whose comments significantly improved this paper. The research was carried out as part of the United Nations University-ITC School for Disaster Geo-Information Management (www.itc.nl/unu/dgim).

References

- Aguilar, F.J., F. Aguera, M.A. Aguilar, and F. Carvajal, 2005. Effects of terrain morphology, sampling density, and interpolation methods on grid DEM accuracy. *Photogrammetric Engineering & Remote Sensing*, 71(7):805–816.

- Aguilar, F.J., F. Aguera, and M.A. Aguilar, 2007. A theoretical approach to modeling the accuracy assessment of digital elevation models, *Photogrammetric Engineering & Remote Sensing*, 73(12):1367–1379.
- Ahmed, N., A. Mahtab, R. Agrawal, P. Jayaprasad, S.K. Pathan, Ajai, D.K. Singh, and A.K. Singh, 2007. Extraction and validation of Cartosat-1 DEM, *Journal of the Indian Society of Remote Sensing*, 35(2):121–127.
- Bahuguna, I.M., A.V. Kulkarni, and S. Nayak, 2004. DEM from IRS-1C PAN stereo coverages over Himalayan glaciated region - Accuracy and its utility, *International Journal of Remote Sensing*, 25(19):4029–4041.
- Bahuguna, I.M., A.V. Kulkarni, and S. Nayak, 2008. Impact of slope on DEM extracted from IRS 1C PAN stereo images covering Himalayan glaciated region: A few case studies, *International Journal of Geoinformatics*, 4(2):21–28.
- Baltsavias, E., S. Kocaman, D. Akca, and K. Wolff, 2007. Geometric and radiometric investigations of Cartosat-1 data, *Proceedings of the ISPRS Workshop -High Resolution Earth Imaging for Geospatial Information*, 29 May-01 June, Hannover, Germany, unpaginated CD-ROM.
- Berthier, E., and T. Toutin, 2008. SPOT5-HRS digital elevation models and the monitoring of glacier elevation changes in North-West Canada and South-East Alaska, *Remote Sensing of Environment*, 112(5):2443–2454.
- Bolstad, P.V., and T. Stowe, 1994. An evaluation of DEM accuracy: Elevation, Slope, and Aspect, *Photogrammetric Engineering & Remote Sensing*, 60(11):1327–1332.
- Carrara, A., M. Cardinali, and F. Guzzetti, 1992. Uncertainty in assessing landslide hazard and risk, *ITC Journal*, 2:172–183.
- Chaplot, V., F. Darboux, H. Bourennane, S. Legu  dois, N. Silvera, and K. Phachomphon, 2006. Accuracy of interpolation techniques for the derivation of digital elevation models in relation to landform types and data density, *Geomorphology*, 77(1–2):126–141.
- Eckert, S., T. Kellenberger, and K. Itten, 2005. Accuracy assessment of automatically derived digital elevation models from aster data in mountainous terrain, *International Journal of Remote Sensing*, 26(9):1943–1957.
- Ehsani, A.H., and F. Quiel, 2008. Application of self organizing map and SRTM data to characterize yardangs in the Lut desert, Iran, *Remote Sensing of Environment*, 112(7):3284–3294.
- Endreny, T.A., E.F. Wood, and D.P. Lettenmaier, 2000. Satellite-derived digital elevation model accuracy: Hydrogeomorphological analysis requirements, *Hydrological Processes*, 14(1):1–20.
- FGDC, 1998. *Geospatial Positioning Accuracy Standards, Part 3: National Standard for Spatial Data Accuracy*, U.S. Federal Geographic Data Committee, URL: <http://www.fgdc.gov/standards/projects/FGDC-standards-projects/accuracy/part3> (last date accessed: 23 January 2010).
- Florinsky, I.V., 1998. Combined analysis of digital terrain models and remote sensing data in landscape investigations, *Progress in Physical Geography*, 22(1):33–60.
- Gong, J., Z. Li, Q. Zhu, H. Sui, and Y. Zhou, 2000. Effects of various factors on the accuracy of DEMs: An intensive experimental investigation, *Photogrammetric Engineering & Remote Sensing*, 66(9):1113–1117.
- Gooch, M.J., J.H. Chandler, and M. Stojic, 1999. Accuracy assessment of digital elevation models generated using the ERDAS Imagine OrthoMAX digital photogrammetric system, *The Photogrammetric Record*, 16(93):519–531.
- Gorokhovich, Y., and A. Voustianiouk, 2006. Accuracy assessment of the processed SRTM-based elevation data by CGIAR using field data from USA and Thailand and its relation to the terrain characteristics, *Remote Sensing of Environment*, 104(4):409–415.
- Gruen, A., S. Kocaman, and K. Wolff, 2007. High Accuracy 3D Processing of Stereo Satellite Images in Mountainous Areas, URL: <http://www.photogrammetry.ethz.ch/general/persons/sultan.html> (last date accessed: 23 January 2010).
- Hirano, A., R. Welch, and H. Lang, 2003. Mapping from ASTER stereo image data: DEM validation and accuracy assessment, *ISPRS Journal of Photogrammetry and Remote Sensing*, 57(5–6):356–370.
- H  hle, J., and M. Potuckova, 2006. The EuroSDR Test “Checking and Improving of Digital Terrain Models” (Official publication No. 51), URL: <http://bono.hostireland.com/~eurosdr/publications/51.pdf> (last date accessed: 23 January 2010).
- Holmes, K.W., O.A. Chadwick, and P.C. Kyriakidis, 2000. Error in a USGS 30-meter digital elevation model and its impact on terrain modeling, *Journal of Hydrology*, 233(1–4):154–173.
- Hu, Y., and C.V. Tao, 2002. Updating solutions of the rational function model using additional control information, *Photogrammetric Engineering & Remote Sensing*, 68(7):715–723.
- Kerle, N., 2002. Volume estimation of the 1998 flank collapse at Casita volcano, Nicaragua: A comparison of photogrammetric and conventional techniques, *Earth Surface Processes and Landforms*, 27(7):759–772.
- Kratky, V., 1989. Rigorous photogrammetric processing of SPOT images at CCM Canada, *ISPRS Journal of Photogrammetry and Remote Sensing*, 44(2):53–71.
- Li, Z., 1991. Effects of check points on the reliability of DTM accuracy estimates obtained from experimental tests, *Photogrammetric Engineering & Remote Sensing*, 57(10):1333–1340.
- Li, Z., Q. Zhu, and C. Gold, 2005. *Digital Terrain Modeling Principles and Methodology*, CRC Press, New York, 323 pp.
- Light, D.L., D. Brown, A. Colvocoresses, F. Doyle, M. Davies, A. Ellasal, J. Junkins, J. Manent, A. McKenney, R. Undrejka, and G. Wood, 1980. Satellite photogrammetry, *Manual of Photogrammetry - Fourth edition* (C.C. Slama, C. Theurer, and S.W. Henriksen, editors), American Society for Photogrammetry and Remote Sensing, Bethesda, Maryland, pp. 883–977.
- Malleswara Rao, T.C., K. Venugopala Rao, A. Ravi Kumar, D.P. Rao, and B.L. Deekshatulu, 1996. Digital Terrain Model (DTM) from Indian Remote Sensing (IRS) satellite data from the overlap area of two adjacent paths using digital photogrammetric techniques, *Photogrammetric Engineering & Remote Sensing*, 62(6):727–731.
- Murphy, M.A., and W.P. Burgess, 2006. Geometry, kinematics, and landscape characteristics of an active transition zone, Karakoram fault system, Southwest Tibet, *Journal of Structural Geology*, 28(2):268–283.
- Murphy, P.N.C., J. Ogilvie, F.-R. Meng, and P. Arp, 2008. Stream network modelling using lidar and photogrammetric digital elevation models: A comparison and field verification, *Hydrological Processes*, 22:1747–1754.
- NRSC, 2006. Cartosat-1 data user’s handbook, URL: http://www.nrsc.gov.in/IRS_Documents/Handbook/cartosat1.pdf (last date accessed: 23 January 2010).
- Radhika, V.N., B. Kartikeyan, B. Gopala Krishna, S. Chowdhury, and P.K. Srivastava, 2007. Robust stereo image matching for spaceborne imagery, *IEEE Transactions on Geoscience and Remote Sensing*, 45(9):2993–3000.
- Sadasiva, Rao, B., A.S.R.K.V. Murali Mohan, K. Kalyanaraman, and K. Radhakrishnan, 2006. Evaluation of Cartosat-I stereo data of Rome, *Proceedings of the International Symposium on Geospatial Databases for Sustainable Development*, 25–30 September, Goa, India, unpaginated CD-ROM.
- Smith, M.J., J. Rose, and S. Booth, 2006. Geomorphological mapping of glacial landforms from remotely sensed data: An evaluation of the principal data sources and an assessment of their quality, *Geomorphology*, 76(1–2):148–165.
- Tao, C.V., and Y. Hu, 2002. 3D Reconstruction methods based on Rational Function Model, *Photogrammetric Engineering & Remote Sensing*, 68(7):705–714.
- Toutin, T., 2001. Elevation modelling from satellite visible and infrared (VIR) data, *International Journal of Remote Sensing*, 22(6):1097–1125.
- Toutin, T., 2004a. Comparison of stereo-extracted DTM from different high-resolution sensors: SPOT-5, EROS-A, IKONOS-II, and QuickBird, *IEEE Transactions on Geoscience and Remote Sensing*, 42(10):2121–2129.
- Toutin, T., 2006. Generation of DSMs from SPOT-5 in-track HRS and across-track HRG stereo data using spatiotriangulation and autocalibration, *ISPRS Journal of Photogrammetry and Remote Sensing*, 60(3):170–181.

- Toutin, T., 2008. ASTER DEMs for geomatic and geoscientific applications: A review, *International Journal of Remote Sensing*, 29(7):1855–1875.
- Van Den Eeckhaut, M., J. Poesen, G. Verstraeten, V. Vanacker, J. Nyssen, J. Moeyersons, L.P.H. van Beek, and L. Vandekerckhove, 2007. Use of LIDAR-derived images for mapping old landslides under forest, *Earth Surface Processes and Landforms*, 32(5):754–769.
- Weibel, R., and M. Heller, 1991. Digital terrain modelling, *Geographical Information Systems, Principles and Applications*, Vol. 1 (D.J. Maguire, M.F. Goodchild, and D.W. Rhind, editors), Longman, Harlow, pp. 269–297.
- Westaway, R.M., S.N. Lane, and D.M. Hicks, 2001. Remote sensing of clear-water, shallow, gravel-bed rivers using digital photogrammetry, *Photogrammetric Engineering & Remote Sensing*, 67(11):1271–1281.
- Wise, S., 2000. Assessing the quality for hydrological applications of digital elevation models derived from contours, *Hydrological Processes*, 14(11–12):1909–1929.
- Wise, S.M., 2007. Effect of differing DEM creation methods on the results from a hydrological model, *Computers and Geosciences*, 33:1351–1365.
- Zhang, L., and A. Gruen, 2006. Multi-image matching for DSM generation from IKONOS imagery, *ISPRS Journal of Photogrammetry and Remote Sensing*, 60(3):195–211.
- (Received 21 October 2008; accepted 24 July 2009; final version 17 August 2009)

2010 *PE&RS* OFFPRINT ORDER FORM

This is the **ONLY** opportunity available to order additional offset printing quality copies of your article. *PE&RS* does not go back on press after the issue's publication. Offprints are only shipped when ordered; they are not complimentary. However, all authors will receive one complimentary copy of the *PE&RS* issue containing their article. This form should be completed as soon as the initial proof is received, and should be returned with payment for offprints and page charges to the Production Manager as indicated below

ARTICLE DESCRIPTION:

ARTICLE TITLE: _____

AUTHOR(S): _____

Please refer to the price chart and conditions on the back of this form in order to complete the table below.

Quantity	Description	Amount
	Offprints	
	Journal Covers (actual issue cover)	
	Extra Pages @ \$125 per page (each page over 7 journal pages, reference "Instructions to Authors")	
	Electronic copy of article in PDF format @ \$2.00 per page Will be emailed. No shipping charges.	
	Shipping (applies to offprints and covers only (see price chart and conditions on back of this form.))	
TOTAL		

SHIPPING ADDRESS:

Name (please print): _____

Organization Name (if applicable): _____

Street Address: _____

City: _____ State/Province: _____ Zip Code/Postal Code: _____

Country: _____ E-mail: _____

Business Phone: _____ Business Fax: _____

METHOD OF PAYMENT:

Payments must be made in US dollars, drawn on a US bank, or appropriate credit card. Make checks payable to ASPRS. Keep a copy for your records.

Visa MasterCard Discover American Express

Check (print *PE&RS* issue date & manuscript # on check)

Name on Credit Card

Account Number

Expires (MO/YR)

Signature

Date

Phone number for person above

SEND THIS FORM ALONG WITH METHOD OF PAYMENT TO:
Production Manager, ASPRS, 5410 Grosvenor Lane, Suite 210, Bethesda, MD 20814-2160
Phone: 301-493-0290 x107, Fax: 301-493-0208

CONDITIONS:

Offprints are only shipped when ordered; they are not complimentary. However, all authors will receive one complimentary copy of the *PE&RS* issue containing their article. Offprint prices are based on the number of pages in an article. Orders are restricted to the quantities listed below. If offprints are not ordered prior to the issue's publication, reprints may be provided in multiples of 100 at the customer's expense. Shipping prices are based on weight and must be added to offprint and journal cover prices for an order to be processed. If overnight delivery is required, customers must provide an account code for the expense of the service (please indicate carrier and account number in the itemized table next to "Shipping").

PRICES:

Please enter the price that corresponds to the quantity of offprints and/or covers being ordered on the front of this form.

Offprints and Covers	25	50	75	100*
Offprints (1 to 4 page article)	9.00	15.00	21.00	27.00
Offprints (5 to 8 page article)	15.00	27.00	39.00	51.00
Offprints (9 to 12 page article)	21.00	39.00	57.00	75.00
Offprints (13 to 16 page article)	27.00	51.00	75.00	99.00
Journal Covers	15.00	25.00	35.00	45.00
Cover sponsor Applies to Outside Front Cover image suppliers only	475.00 for 1000 covers and TOC			

*Additional offprints can be ordered in the increments listed above for the prices listed. When ordering additional offprints, add 25% to postage costs listed below.

POSTAGE:

Please enter the price that corresponds to the quantity of offprints and/or covers being ordered on the front of this form.

Domestic (UPS Ground)	25	50	75	100	Canada (Air Parcel Post)	25	50	75	100
Offprints (1-4 page article)	7.59	7.98	9.08	8.69	Offprints (1-4 page article)	19.14	20.78	21.45	22.11
Offprints (5-8 page article)	7.98	9.08	9.57	10.53	Offprints (5-8 page article)	20.68	22.11	22.11	23.87
Offprints (9-12 page article)	8.25	9.57	9.79	10.23	Offprints (9-12 page article)	21.45	23.87	26.57	28.82
Offprints (13-16 page article)	8.69	9.79	10.23	11.44	Offprints (13-16 page article)	22.11	25.74	28.82	31.96
Journal Covers	7.59	7.98	8.25	8.64	Journal Covers	19.14	20.68	21.45	22.11
Cover sponsor Applies to Outside Front Cover image suppliers only	70.00				Cover sponsor Applies to Outside Front Cover image suppliers only	Contact ASPRS for shipping prices.			
Mexico (Air Parcel Post)	25	50	75	100	Overseas (Air Parcel Post)	25	50	75	100
Offprints (1-4 page article)	22.39	23.87	24.75	27.12	Offprints (1-4 page article)	28.05	30.31	41.69	36.03
Offprints (5-8 page article)	24.11	27.12	30.64	34.50	Offprints (5-8 page article)	30.36	36.03	45.26	47.41
Offprints (9-12 page article)	25.52	30.69	36.03	40.26	Offprints (9-12 page article)	33.17	41.69	49.55	55.99
Offprints (13-16 page article)	27.12	34.60	40.26	45.98	Offprints (13-16 page article)	36.03	47.41	55.99	64.51
Journal Covers	22.33	23.87	25.52	27.12	Journal Covers	28.05	30.31	41.69	36.03
Cover sponsor Applies to Outside Front Cover image suppliers only	Contact ASPRS for shipping prices.				Cover sponsor Applies to Outside Front Cover image suppliers only	Contact ASPRS for shipping prices.			

Assignment of Copyright to ASPRS

Current copyright law requires that authors of papers submitted for publication in *Photogrammetric Engineering & Remote Sensing* transfer copyright ownership to the American Society for Photogrammetry and Remote Sensing before the paper may be published. Upon receipt of this form with your Master Proof, please complete this form and forward it to the Production Coordinator (address below).

Manuscript Title: _____

Author(s): _____

Assignment of Copyright in the above-titled work is made on (date) _____ from the above listed author(s) to the American Society for Photogrammetry and Remote Sensing, publisher of *Photogrammetric Engineering & Remote Sensing*.

In consideration of the Publisher's acceptance of the above work for publication, the author or co-author(s) hereby transfer(s) to the American Society for Photogrammetry and Remote Sensing the full and exclusive copyright to the work for all purposes for the duration of the copyright. I (we) understand that such transfer of copyright does not preclude specific personal use, provided that prior to said use, permission is requested from and granted by the American Society for Photogrammetry and Remote Sensing.

I (we) acknowledge that this paper has not been previously published, nor is it currently being considered for publication by any other organization.

Author/co-author signatures

Co-authors may fill out and submit this form separately (photocopies are acceptable) if desired; but all co-authors must sign either this or a separate form.

Special Note to U.S. Government Employees

Material prepared by U.S. Government employees as part of their official duties need not have the assignment of copyright transferred since such material is automatically considered as part of the public domain.

If your paper falls within this category please check the appropriate statement and sign below.

_____ This paper has been prepared wholly as part of my (our) official duties as (a) U.S. Government Employee(s). I (we) acknowledge that this paper has not previously been published, nor is it currently being considered for publication, by any other organization.

_____ This paper has been prepared partly in the course of my (our) official duties as (a) U.S. Government Employee(s). For any part(s) not prepared in the course of my (our) official duties, copyright is hereby transferred to the American Society for Photogrammetry and Remote Sensing. I (we) acknowledge that this paper has not previously been published, nor is it currently being considered for publication, by any other organization.

Author/co-author signatures

Please return this form to:
Production Coordinator, ASPRS
5410 Grosvenor Lane, Suite 210
Bethesda, MD 20814-2160
301-493-0290, 301-493-0208 (fax), www.asprs.org

2010 *PE&RS* COLOR ORDER FORM

Accepted manuscripts will not be released for publication until all color charges have been paid. Color payment should be made when final manuscript is returned for publication to the Manuscript Coordinator. Payment and this form must be mailed/faxed to the ASPRS Production Manager at the address below.

ARTICLE DESCRIPTION:

ARTICLE TITLE: _____

AUTHOR(S): _____

MANUSCRIPT # (if applicable): _____ # OF COLOR IMAGES/FIGURES: _____

COLOR PRICES AND CONDITIONS:

	1	2	+ **
Color Plates in Manuscripts (quantity _____) *	1,000.00	1,650.00	575.00
Outside Front Cover (discounts for reserving more than one cover at a time. 50% non-refundable deposit is required at time of reservation.)	3,300.00		

* For purposes of this form, a color plate is considered to be a plate that is numbered, even if it contains several parts, e.g. (a), (b), and so on.
**There is a \$575.00 per plate charge for each color plate over two (2).

Quantity	Description	Amount
	Color Plates (# of pages with color images/figures)	
	Cover Image (50% deposit required at time of reservation)	
TOTAL		

METHOD OF PAYMENT:

Accepted manuscripts with color images will not be released for publication until this form is received along with payment. Payments must be made in US dollars, drawn on a US bank, or appropriate credit card. Make checks payable to ASPRS. Keep a copy for your records.

Visa MasterCard Discover American Express

Check (print *PE&RS* issue date & manuscript # on check)

Name on Credit Card

Account Number

Expires (MO/YR)

Signature

Date

Phone number for person above

Name/Contact Information of author submitting this form:

Name: _____

Affiliation: _____

Address: _____

Phone: _____

Fax: _____

Email: _____

SEND THIS FORM ALONG WITH METHOD OF PAYMENT TO:

Production Manager, ASPRS, 5410 Grosvenor Lane, Suite 210, Bethesda, MD 20814-2160
301-493-0290 x107, 301-493-0208 (fax)